Oxygen incorporation effects in annealed epitaxial $La_{(1-x)}Sr_xMnO_3$ thin films

T. Petrisor, Jr.,[1,2,a)] M. S. Gabor[1,2] A. Boulle,[3] C. Bellouard,[2] C. Tiusan,[1,2] O. Pana,[4] and T. Petrisor[1]

[1]*Technical University of Cluj-Napoca, Str. Memorandumului, nr. 28, 400114 Cluj-Napoca, Romania*
[2]*Institut Jean Lamour, UMR 7198 CNRS-Nancy Université, Vandœuvre-les-Nancy, France*
[3]*Science des Procédés Céramiques et de Traitements de Surface (SPCTS), CNRS UMR 6638, Centre Européen de la Céramique, 12 rue Atlantis, 87068 Limoges, France*
[4]*National Institute for Research and Development of Molecular and Isotopic Technologies, P.O. Box 700, 400293, Cluj-Napoca, Romania*

(Received 23 February 2011; accepted 2 May 2011; published online 21 June 2011)

This paper presents our results regarding oxygen incorporation effects in epitaxial $La_{(1-x)}Sr_xMnO_3$ thin films, deposited on $SrTiO_3$ (001) single crystal substrates, by annealing in different gas mixtures of argon and oxygen. A particular emphasis is placed on the correlation of structural properties with the magnetic properties of the films, Curie temperature, and coercive field. In this sense, we demonstrate that the evolution of the diffuse part of the ω-scans performed on the films are due to oxygen excess in the film lattice, which creates cationic vacancies within the films. Also, we show that two regimes of oxygen incorporation in the films exist, one in which the films evolve toward a single phase and oxygen stoichiometry is recovered, and a second one dominated by oxygen over-doping effects. In order to support our study, XPS measurements were performed, from which we have evaluated the Mn^{3+}/Mn^{4+} ionic ratio. © *2011 American Institute of Physics*. [doi:10.1063/1.3596807]

I. INTRODUCTION

Doped rare earth manganite thin films have attracted a lot of attention from the scientific community over the last two decades due to the advent of spintronics and the search for new materials with properties suited for spintronic device fabrication.[1] High spin polarization and the colossal magnetoresistive (CMR) effect[2] recommend these systems as worthy candidates for applications in the field of magnetic sensing. As has been established since their discovery in the 1950s, the ferromagnetic phase is stabilized by means of the "double-exchange" mechanism,[3] which consists of an electronic transfer between Mn^{3+} and Mn^{4+} ions via an O^{2-} ion in Mn^{3+}- O^{2-}- Mn^{4+} bonds. It can readily be seen that this mechanism is conditioned by the presence in the lattice of the 4+ valance state of the Mn ion, which is primarily achieved by means of divalent ion doping. Urushibara *et al.*[4] have constructed a magnetic phase diagram of $La_{(1-x)}Sr_xMnO_3$ as a function of Sr doping. They have shown that the wealth of magnetic properties that this material exhibits is governed by the $x/1-x$, Mn^{4+}/Mn^{3+} ion ratio. Besides doping, this ratio can be finely tuned by means of excess oxygen incorporation in the lattice. Roosmalen *et al.*[5] have constructed a defect model for the end member, $LaMnO_3$, when it is subjected to an oxygen over-doping, d. Their model, applied to $La_{(1-x)}Sr_xMnO_3$ (LSMO), is summarized, using the Kröger-Vink notation, by the following equation:

$$6Mn_{Mn} + \frac{3}{2}O_2(g) \rightarrow V'''_{Mn} + V''''_{Mn} + V'''_{La} + V''_{Sr} + 6Mn^{\bullet}_{Mn} + La_{(1-x)}Sr_xMnO_3 \quad (1)$$

Thus, an excess d of oxygen produces an equal amount of cationic La, Sr, and Mn vacancies, denoted by V and the appropriate negative charge, ($'$), while also increasing the number of Mn^{4+} ions and changing the Mn^{4+}/Mn^{3+} ionic ratio accordingly, to $(x+2d)/(1-x-2d)$. In the above equation the Mn^{3+} state was considered to be neutral, which resulted in Mn^{4+} having only one extra positive charge, denoted by ($^{\bullet}$). There have been a quite a number of papers dealing with the effects of oxygen excess in doped lanthanum manganites, usually attained by means of high temperature annealing in oxygen atmosphere, on the structural, magnetic, and electric properties of epitaxial manganite thin films.[6–8] These studies show that upon oxygen annealing the out-of-plane lattice parameter shows a decrease as the Mn^{4+} ionic radius is lower than the Mn^{3+} one,[6] accompanied by a decrease of the magnetic moment/Mn ion,[7] and, especially for cationic under-doped samples, an increase of the Curie and metal-insulator transition temperatures.[8]

In the present paper we have set out to study the effects of excess oxygen incorporation in the lattice of epitaxial $La_{(1-x)}Sr_xMnO_3$ thin films deposited on (001) $SrTiO_3$ substrates, focusing mainly on the vacancy, i.e., defect, creation and their characterization by means of x-ray diffraction techniques. In order to validate that the defect formation arises from the cationic vacancies produced by oxygen over-doping we have also performed magnetic measurements of the quantities strongly affected by oxygen stoichiometry, Curie temperature,

a)Authors to whom correspondence should be addressed. Electronic mail: traian.petrisorjr@phys.utcluj.ro.

and coercive field, and interpreted the results within the framework set by the aforementioned studies. X-ray photoelectron spectroscopy (XPS) measurements have also been employed for the evaluation of the Mn^{3+}/Mn^{4+} ion ratio.

II. EXPERIMENTAL

The LSMO epitaxial thin films were deposited by means of dc sputtering on (001) $SrTiO_3$ (STO) single crystal substrate in a mixture of Ar and O_2, with a 3:1 ratio at a total pressure of 40 mTorr, from a stoichiometric, 2 in $La_{0.66}Sr_{0.33}MnO_3$ target. The deposition was performed at a substrate temperature of 650 °C. During cooling, at a rate of 10 °C/min, an additional annealing sequence was performed at 550 °C for 30 min in 520 Torr of oxygen atmosphere. In order to study the oxygen incorporation effects in LSMO, the film was cut into pieces of about 5×5 mm^2 which were subsequently annealed at 900 °C for 1 h in flowing annealing gas comprised of an Ar and O_2 mixture in a (100%-x):x ratio, with x taking the values 0%, 3%, 10%, 25%, and 100%. The structural, x-ray characterization of the films was carried out using a Bruker AXS D8 Discover diffractometer in a high resolution x-ray diffraction (HRXRD) configuration. The magnetic characterization was performed using a Quantum Design SQUID magnetometer. The Mn^{3+}/Mn^{4+} of the samples was determined by x-ray photoelectron spectroscopy of the Mn 2p core level lines. Ar^+ ion etching was performed in order to remove contamination layers. The samples were subjected to consecutive etchings until, by performing an additional milling, the measured spectra remained unchanged in shape and intensity.

III. RESULTS AND DISCUSSION

A. HRXRD characterization

Figure 1 shows the evolution of the $2\theta/\omega$ scans of the (002) LSMO peak for the different compositions of the annealing gas. All curves could be fitted with a simple semikinematical film/substrate model.[9] The film and substrate diffract coherently, indicating a high structural quality of the

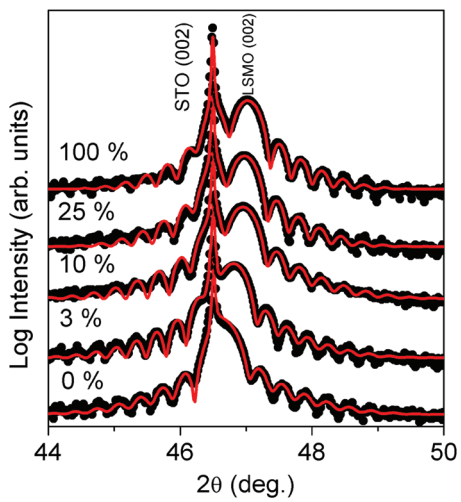

FIG. 1. (Color online) $2\theta/\omega$ scans around the (002) peaks of the LSMO films and STO substrate for different values of $x = 0\%$, 3%, 10%, 25%, and 100% (circles) and the corresponding simulated curves (lines).

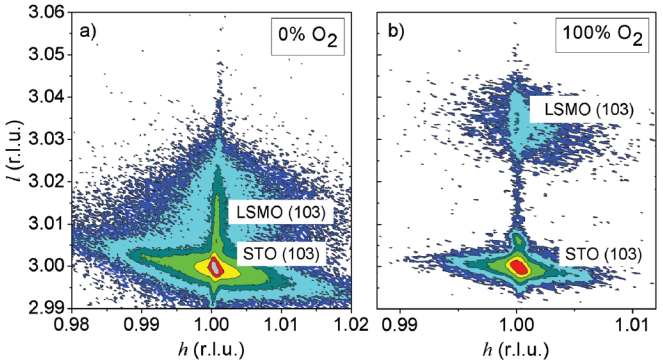

FIG. 2. (Color online) Reciprocal space map around the (103) peaks of the LSMO thin film annealed in (a) 0% and (b) 100% oxygen and of the STO substrate.

films. The film thicknesses are in the 29–31 nm range and the film's roughness is less than 1.2 nm. As the oxygen content of the annealing gas increases one can observe a tendency of the (002) LSMO peak to shift toward higher 2θ values, indication of a decrease of the out-of-plane LSMO lattice parameter, c. The decrease of c is generally regarded as an indication of oxygen incorporation in the LSMO lattice, as the Mn^{3+} valence state changes to Mn^{4+}, which has a lower ionic radius.[6] Dabrowski *et al.*[10] suggested that the decrease in the lattice parameter can be also ascribed to the creation of vacancies in the lattice due to the excess of oxygen. On the other hand, the observed evolution of the c parameter might also be due to an evolution of the state of strain of the film. In order to discriminate between both contributions we recorded reciprocal space maps around the (103) LSMO and STO reflections. In Fig. 2 is shown the reciprocal space map for the films annealed in pure argon and pure oxygen. As it can be seen, the peaks of the film and substrate have the same value of h, namely 1, indicating that the two lattices are perfectly matched in the in-plane direction, having the lattice constant of the STO substrate, 3.905 Å. In all cases the films are fully strained and the corresponding in-plane strain is $e_{xx} = (a_{STO} - a^{bulk}_{LSMO})/a^{bulk}_{LSMO}$. The strain free parameter of LSMO is denoted a^{bulk}_{LSMO}, so as to distinguish it from the measured (strained) values a and c. Since the same result was found to be true for all the annealed samples, this is a clear indication that the observed evolution of the c parameter is solely related to compositional changes, namely oxygen content.

The influence of the oxygen content on the in-plane and out-of-plane lattice parameter is presented in Fig. 3. We deduce the influence of the oxygen incorporation only, i.e., without the effect of strain, according to $a^{bulk}_{LSMO} = (c + \nu_2 a_{STO})/(1 + \nu_2)$, where ν_2 is the biaxial Poisson's ratio which is related to the uniaxial Poisson's ratio through $\nu_2 = 2\nu/(1 - \nu)$. In the case of LSMO we have $\nu = 0.4$,[11] and the parameter c is obtained either from the reciprocal space map (Fig. 2) or from the $2\theta/\omega$ scan (Fig. 1). It can be seen that the strain free lattice parameter decreases as a function of the oxygen content in the treatment gas, following two regimes. The first, up to 10%, is characterized by strong decrease of the lattice parameter, indicating a pronounced oxygen incorporation effect in the film lattice. In the second

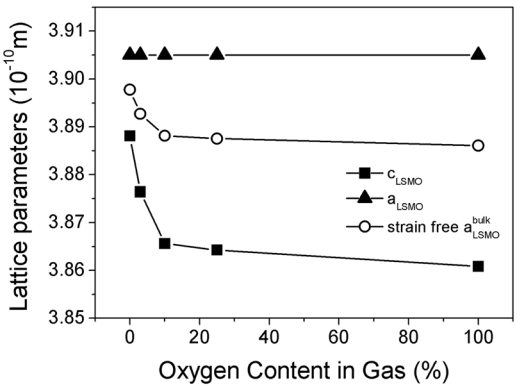

FIG. 3. LSMO thin films lattice parameters evolution as a function of the oxygen content in the annealing gas.

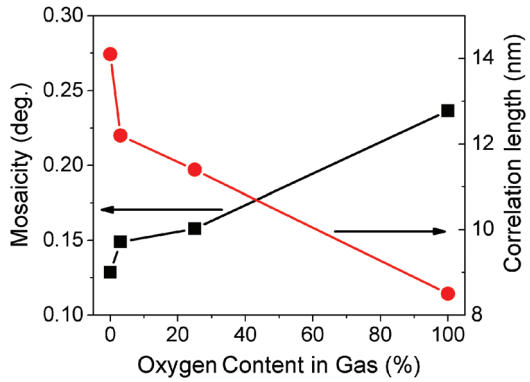

FIG. 5. (Color online) Evolution of the mosaicity and correlation length of the defects, as obtained by fitting the rocking curves around the (002) and (001) peaks of the LSMO films.

regime, from 10% to 100% oxygen content, the lattice parameter exhibits only a slight decrease. The overall behavior is similar to the random-defect model in LSMO[12] in which the abrupt decrease corresponds to oxygen incorporation in the oxygen deficient phase, while the mild decrease is due to oxygen over-doping.

The ω-scans around the (002) LSMO peaks of the annealed samples are presented in Fig. 4. All peaks exhibit a profile comprised of a narrow, high intensity component corresponding to the coherent scattering part, and a broad, low intensity component, corresponding to the diffuse scattering part. The two component rocking curves of epitaxial thin films have been observed in a wide variety of thin film systems.[13–15] The presence of the diffuse scattering component stems from the existence of distorted regions (of limited spatial extension) in the film. These regions are situated around defects such as dislocations, grain boundaries, chemical inhomogeneities, etc. The coherent part originates from the long-range order inherent in high-quality crystalline structures. Quantitative information regarding the spatial and statistical properties of the strain field, as well as regarding the in-plane coherence length ("crystallite" size) can be deduced from the numerical simulation of such ω-scans.[16] In the present case a good agreement between the calculated and the observed curves could be obtained assuming a Gaussian distribution of strain and crystallites having a parallelepipedic shape. The strain field is characterized by an in-plane correlation length ξ, below which the lattice displacements are correlated, which in the case of a symmetrical reflection, correspond to the root-mean-squared (r.m.s) rotations, i.e., the mosaicity. This mosaicity gives rise to the diffuse peak. Above the correlation length ξ, the displacements are uncorrelated so that the mosacity drops down to zero, which gives rise to the coherent peak. The correlation length ξ, hence, corresponds to the spatial extension of the strain field which can be often be regarded as a "mean distance" between defects.[17] It must be noted that the simulation of several $(00l)$ reflections is necessary in order to determine the different parameters entering the model. We here used the (001) and (002) reflections. Finally, it is to be noticed that the ω-scan of the film annealed in 10% oxygen could not be simulated properly with the described model, as it exhibited an additional signal, giving rise to two shoulders, indicated by the arrows in Fig. 4. The presence of such distinct features in epitaxial LSMO thin films has been attributed to the presence of periodic microtwinning.[18] The evolution of the mosaicity and the correlation length as a function of oxygen content are presented in Fig. 5. Starting from $x = 3\%$, the correlation length of the defects decreases, while the mosaicity increases. This evolution can be interpreted as follows: as oxygen incorporation in the film lattice increases, due to higher oxygen concentration in the annealing gas, a greater number of cationic vacancies form, according to the defect model, (1). These vacancies act as defects, locally distorting the lattice, giving rise to the diffuse scattering component of the rocking curves. As the defect density increases the mosaicity increases, i.e., the strength of the defects increases. Concomitantly, the distance between defects decreases, i.e., the extension of the distortion field of an individual defect is reduced by the presence of adjacent distortions.

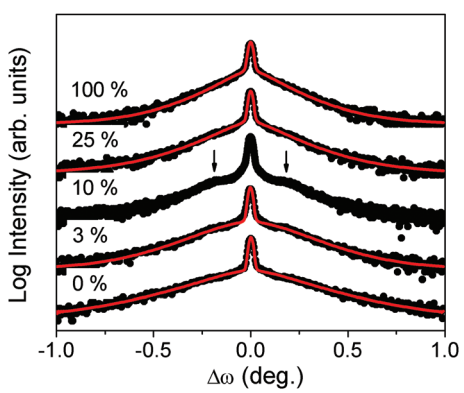

FIG. 4. (Color online) Rocking curves around the (002) peak of the annealed LSMO thin films (circles) and the simulated curves (lines).

B. Magnetic properties and XPS characterization

In order to demonstrate the validity of our interpretation we have conducted a series of magnetic measurements, as well as a XPS investigation on our samples, from which we have evaluated physical quantities that are dependent both on oxygen and defect concentration, such as Curie temperature, T_C; the coercive field; and the Mn^{3+}/Mn^{4+} ionic ratio.

The temperature dependence of the magnetization, M(T), for the annealed films is presented in Fig. 6. From the

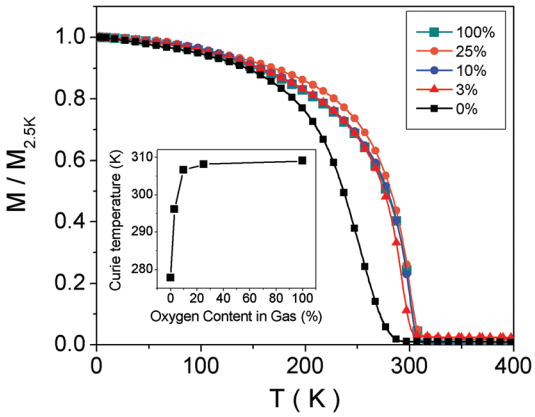

FIG. 6. (Color online) M(T) curves for the annealed samples (some data points were removed for clarity); Curie temperature evolution as a function of the oxygen content in the annealing gas (inset).

derivative of the M(T) curves, the ferromagnetic-paramagnetic transition width was investigated, taking as a parameter the full width at half maximum (FWHM) of the *dM/dT* peak around the inflection point of the M(T) curves, Fig. 7. The behavior of the FWHM also suggests the existence of the two oxygen incorporation regimes, in agreement with the structural studies. Thus, for the films annealed in up to 10% oxygen concentration, the FWHM decreases, i.e., the ferromagnetic-paramagnetic transition becomes narrower as a function of temperature. This behavior can be ascribed to an evolution of the films toward a low defect density and possibly oxygen stoichiometric phase. The large FWHM value of the 0% oxygen content annealed sample is an indication that the film exhibits multiple magnetic phases, having different Curie temperatures. These phases could in turn come from the existence of slight local compositional and/or structural variations within the film. It is to be noted that such local inhomogenities can hardly be evidenced by the HRXRD measurement, which might explain the contradiction between the high value of the coherence length, determined from the ω-scan, and the value of FWHM of the *dM/dT* peak, in the case of the film annealed in pure argon. On the other hand, for oxygen concentrations above 10%, a slight increase of the FWHM is noted. This trend can be interpreted as the effect of oxygen over-doping which

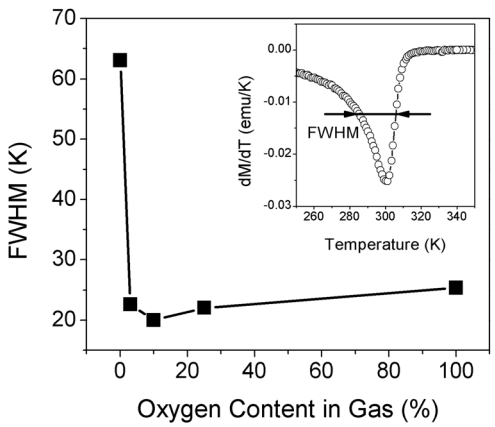

FIG. 7. Full width at half maximum (FWHM) of the *dM/dT* peak around the inflection point of the M(T) curves; *dM/dT* curve for the 10% oxygen annealed film (inset).

creates cationic vacancies in the film crystal structures. Taking into account the above considerations, we can conclude that in the first regime oxygen annealing acts to homogenize the films into a single phase with recovered oxygen stoichiometry, while the second regime is governed by uniform oxygen incorporation in the single phase films, leading to oxygen over-doped, $La_{(1-x)}Sr_xMnO_{3+d}$ films.

The Curie temperatures were determined by linear extrapolation of the M(T) curves around the inflection points and are presented in the inset of Fig. 6. A pronounced increase of T_C is observed from 278 K, corresponding to the film annealed in Ar, to 307 K, for the film annealed in 10% oxygen, as the structure evolves to a single phase possibly having stoichiometric oxygen content. Above 10% oxygen content the increase is slower, reaching a maximum value, for 100% oxygen annealed film, of 309 K. The slight increase observed above 10% oxygen content suggests a hole doping effect of oxygen excess in a sub-optimum ($x < 0.33$) cationic, i.e., strontium, doped phase. A similar effect was also observed by Murugavel *et al.*,[8] in their studies of oxygen annealing effects on cationic under-doped $La_{(1-x)}Ca_xMnO_3$ films, where the dramatic increase of the metal-insulator transition temperature, T_{MI}, from 240 K for the as-deposited to 270 K for oxygen annealed film was ascribed to the effective hole doping originating from oxygen excess in the film lattice. The lack of the exact Sr concentration value of our films prevents us from making any quantitative evaluation of the amount of excess oxygen in the annealed films based on the T_C value. There have also been results[10] on oxygen incorporation effects in LSMO, in which above a certain oxygen doping level, due to the induced structural defects, the Curie temperature experienced a decrease. It seems that in our case, the only slight increase of the Curie temperature is the result of two competing mechanisms. The first, the creation of excess Mn^{4+} ions, would lead to a dramatic increase of the T_C, according to the phase diagram presented by Urushibara *et al.*,[4] while the second, the simultaneous creation of cationic vacancies, would lead to a decrease of T_C, as pointed out by Dabrowski *et al.*,[10] Thus, the overall behavior of the Curie temperature as a function of the oxygen concentration of the annealing gas, above 10% oxygen content, results only in a slight increase.

As far as the coercive field of the LSMO films is concerned, Sirena *et al.*[19] studied the effect of oxygen incorporation in LSMO thin films, which were initially oxygen deficient, on the coercive field. They concluded that upon oxygen annealing, the coercive field of the films decreases. Considering domain wall pinning on structural defects as the main mechanism of coercivity, they attributed their result to the fact that oxygen incorporation in oxygen deficient samples results in a reduction of the number of oxygen vacancies, i.e., structural defects, thus leading to a reduction of coercive field. The evolution of the coercive field as a function of the annealing conditions is given in Fig. 8, evaluated from hysteresis loops performed at 5 K. The coercive field decreases from a value of 80 Oe for the argon annealed sample, to 35 Oe for the film annealed in 3% oxygen. The coercive field in the case of the 10% film is close to this value,

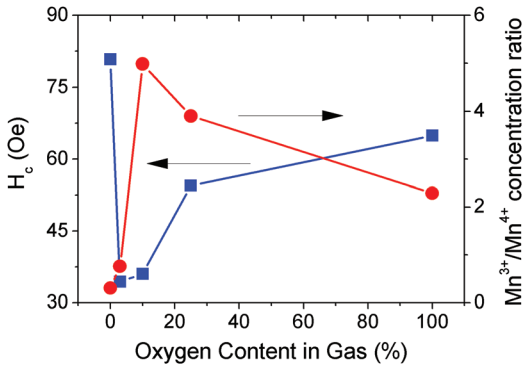

FIG. 8. (Color online) Evolution of the coercive field and of the Mn^{3+}/Mn^{4+} ratio, determined by XPS measurements, as a function of oxygen concentration of the annealing gas.

36 Oe. For the 25% and 100% oxygen annealed films the value of the coercive field increases to 55 Oe and 64 Oe, respectively. Following the arguments used by Sirena *et al.*,[19] we can explain the decrease of the coercive field by the structural evolution of the LSMO thin films toward a single, low defect phase, up to 10%. For the 25% and 100% films the increase of the coercive field is related to the increase of the defect density due to oxygen over-doping, as revealed by the decrease of the coherence length, seen in Fig. 5. The existence of the oxygen over-doping regime is also confirmed by the XPS measurements that we have performed on the annealed samples. From the fitting of the obtained XPS spectra the Mn^{3+}/Mn^{4+} ionic ratio in the films was determined (Fig. 8). A decrease of the ionic ratio is observed starting from the 10% oxygen annealed film. This is in good agreement with the previous findings, in the sense that the increase of the Mn^{4+} ionic fraction is due to the presence of excess oxygen in the film lattice.[5] The origin of the increase of the ionic ratio for the films annealed in 0% and 3% oxygen remains unclear, even though the high concentration of Mn^{4+} in the 0% film can be attributed to the fact that the film is a mixture of LSMO phases, and therefore Mn^{4+} rich regions may exist within the film.

IV. CONCLUSION

This paper presents the influence of oxygen incorporation on thin epitaxial LSMO films grown on STO (001) substrates by annealing in mixtures of argon and oxygen atmosphere with different O_2/Ar ratios. Our studies show that two regimes of oxygen incorporation in the film lattice exist. The first, for low concentration of oxygen in the annealing gas, up to 10%, is characterized by the evolution of the films toward a single phase and a rather high rate of oxygen incorporation, as evidenced by the large variation of the measured physical quantities. The second one, for high oxygen concentration in the annealing gas, is a regime in which oxygen is present in excess in the film lattice, leading to the creation of cationic vacancies with specific effects on the physical properties of the films. We have shown that the cationic vacancies created by the presence of excess oxygen in the lattice are correlated with the existence and the evolution of the diffuse scattering part of the ω-scan around the $(00l)$ peaks of the films. Finally, we have shown that the physical properties of LSMO thin films can be modulated by post-deposition annealing in different oxygen concentration of the annealing gas, which is important for future applications of the LSMO thin films.

ACKNOWLEDGMENTS

This work has been partially supported by CNCSIS (National Council for Scientific Research and Higher Education) UEFISCSU (Executive Unit for Higher Education and University Scientific Research Financing), project number PNII IDEI No. 4/2010, code ID-106 and by POS CCE ID. 574, code SMIS-CSNR 12467.

[1]K. Dörr, J. Phys. D **39**, R125 (2005); J.A.-M. Haghiri-Gosnet and J.-P. Renard, J. Phys. D **36**, R127 (2003).
[2]S. Jin, T. H. Tiefel, M. Mc Cormack, R. A. Fastnacht, R. Ramesh, and L. H. Chen, Science **264**, 413 (1994).
[3]C. Zener, Phys. Rev. **82**, 403 (1951); C. Zener, Phys. Rev. B **81**, 440 (1951).
[4]A. Urushibara, Y. Moritomo, T. Arima, A. Asamitsu, G. Kido, and Y. Tokura, Phys. Rev. B **51**, 14103 (1995).
[5]J. A. M. van Roosmalen, E. H. P. Cordfunke, R. B. Helmholdt, and H. W. Zandbergen, J. Solid State Chem. **110**, 100 (1994); J. A. M. van Roosmalen and E. H. P. Cordfunke, J. Solid State Chem. **110**, 106 (1994); J. A. M. van Roosmalen and E. H. P. Cordfunke, J. Solid State Chem. **110**, 109 (1994); J. A. M. van Roosmalen and E. H. P. Cordfunke, J. Solid State Chem. **110**, 113 (1994).
[6]Y. S. Du, B. Wang, T. Li, D. B. Yu, and H. Yan, J. Magn. Magn. Mater. **297**, 88 (2006).
[7]W. Prellier, M. Rajesawi, T. Venkatesan, and R. L. Greene, Appl. Phys. Lett. **75**, 1446 (1999).
[8]P. Murugavel, J. H. Lee, J.-G. Yoon, T. W. Noh, J.-S. Chung, M. Heu, and S. Yoon, Appl. Phys. Lett. **82**, 1908 (2003).
[9]A. Boulle, F. Conchon, and R. Guinebretiere, J. Appl. Crystallogr. **42**, 85 (2009).
[10]Dabrowski, B., R. Dybzinski, Z. Bukowski, O. Chmaissen, and J. D. Jorgensen, J. Solid State Chem. **146**, 448 (1996).
[11]A. Tebano, A. Orsini, P. G. Medaglia, and G. Balestrino, Appl. Phys. Lett. **94**, 242503 (2009).
[12]J. Nowotny and M. Rekas, J. Am. Ceram. Soc. **81**, 67 (1998).
[13]H. Heineke, V. Kirchner, H. Selke, R. Chierchia, R. Ebel, S. Einfeldt, and D. Hommel, J. Phys. D: Appl. Phys. **34**, A25 (2001).
[14]T.-B. Hur, Y.-H. Hwang, H.-K. Kim, and H.-L. Park, J. Appl. Phys. **96**, 1740 (2004).
[15]M. J. Bentall, R. A. Cowley, R. C. C. Ward, M. R. Wells, and A. Stunault, J. Phys.: Condens. Matter **15**, 7155 (2003).
[16]A. Boulle, R. Guinebretiere, and A. Dauger, J. Phys. D: Appl. Phys. **38**, 3907 (2005).
[17]A. Boulle, R. Guinebretiere, and A. Dauger, J. Appl. Phys. **97**, 073503 (2005).
[18]U. Gebhardt, N. V. Kasper, A. Vigliante, P. Wochner, H. Dosch, F. S. Razavi, and H.-U. Habermeier, Phys. Rev. Lett. **98**, 096101 (2007); S. W. Jin, G. Y. Gao, Z. Huang, Z. Z. Yin, X. Zheng, and W. Wu, Appl. Phys. Lett. **92**, 261901 (2008).
[19]M. Sirena, N. Haberkorn, M. Granada, L. B. Steren, and J. Guimpel, J. Magn. Mag. Mater. **272**, 1171 (2004).